X-ray scattering study of the incommensurate phase in Mg-doped $CuGeO_3$

R. J. Christianson,[1] Y. J. Wang,[1] S. C. LaMarra,[1] and R. J. Birgeneau[1,2]
[1]*Department of Physics, Massachusetts Institute of Technology, Cambridge, Massachusetts 02139*
[2]*Department of Physics, University of Toronto, Toronto, Ontario, Canada M5S 1A7*

V. Kiryukhin
Department of Physics and Astronomy, Rutgers University, Piscataway, New Jersey 08854

T. Masuda, I. Tsukada, and K. Uchinokura
Department of Applied Physics, University of Tokyo, 7-3-1 Hongo, Bunkyo-ku, Tokyo 113-8656, Japan

B. Keimer
Max-Planck-Institute für Festkörperforschung, D-70569 Stuttgart, Germany
(Received 28 June 2002; published 11 November 2002)

We present results of a systematic x-ray scattering study of the effects of Mg doping on the high-field incommensurate phase of $CuGeO_3$. Lorentzian-squared line shapes, the changing of the first-order transition to second order, and the destruction of long-range order with infinitesimal doping are observed, consistent with random-field effects in a three-dimensional XY system. Values for the soliton width in pure and lightly doped $CuGeO_3$ are deduced. We find that even a very small doping has a drastic effect on the shape of the lattice modulation.

DOI: 10.1103/PhysRevB.66.174105 PACS number(s): 64.70.Rh, 61.72.Ww, 61.10.Nz

I. INTRODUCTION

The spin-Peierls phase is a novel state of matter consisting of coupled magnetic and structural order parameters.[1] One-dimensional Heisenberg magnetic systems cannot order due to the effects of fluctuations. However, chains of antiferromagnetically coupled quantum spin-$\frac{1}{2}$ ions which are arrayed in a three-dimensional crystal structure can lower their overall energy if the lattice is deformable, allowing neighboring spins within the chains to pull together into a dimerized structure and thereby form spin singlet pairs, a combined magnetic and structural ordering which is known as the spin-Peierls state. The dimerization opens up a gap in the long-wavelength spin excitation spectrum, thus reducing the quantity of fluctuations, and the associated energy. The lowest-energy fluctuations from the dimerized state are unpaired spins known as solitons.

It is not surprising that the spin-Peierls phase, with its intricate coupling between structure and magnetism, should be sensitive to an external magnetic field. As early as 1978 it was predicted that the spin-Peierls transition temperature should decrease with increasing magnetic field,[1] and that when the energy of the spins in the magnetic field exceeds the lattice commensurability energy (Umklapp), solitons should spontaneously form. If these solitons repel each other (as they do), they should form a lattice incommensurate with the crystal structure, with an incommensurability which is proportional to the applied field.[2,3] Since each soliton is accompanied by a structural antiphase domain wall, the incommensurate phase is visible to structural x-ray scattering experiments as a splitting of the spin-Peierls dimerization peak into two peaks displaced along the chain direction.

As has been demonstrated heuristically by Harris *et al.*,[4,5] the spin-Peierls phase can be mapped onto an Ising model, where the up or down pseudospins correspond to the two choices of pairing (left or right) for a given spin. The incommensurate phase, on the other hand, seems to be evidently an XY phase, since the order parameter has two dimensions: the magnitude of the ordering and the phase of the incommensurability.

Until 1993, all of the materials which were known to display a spin-Peierls transition were organic. This made it very difficult to carry out systematic studies. It was generally difficult to grow high-quality large single crystals of the organic materials and the organics tended to be easily damaged by x-ray radiation, which meant that studies of the structure were mostly limited to lower resolution neutron scattering measurements.

In 1993, Hase *et al.*[6] discovered that $CuGeO_3$ was a spin-Peierls system, with a transition at around 14.3 K. This discovery initiated a renewed flurry of experimental activity surrounding the spin-Peierls transition. Particularly, the access to an inorganic spin-Peierls system opened up the possibility of controlled study of the effects of disorder on the spin-Peierls state. The growth defects in the organic materials, as well as the damage caused by x-ray radiation, tended to act as uncontrolled and uncharacterizable sources of disorder. Consistent results for pure samples were therefore difficult to obtain, and it was even more difficult to characterize the effects of a given doping. $CuGeO_3$, on the other hand, was simple to grow with few defects and was not significantly damaged by x-ray radiation, making the level of unintentional defects small.

The high-field incommensurate state was directly observed in $CuGeO_3$ using x-ray scattering by Kiryukhin *et al.*[7] Shortly thereafter, they published a study of the effects of doping on the incommensurate state.[8] In this work, we expand upon the results presented in their paper to try to con-

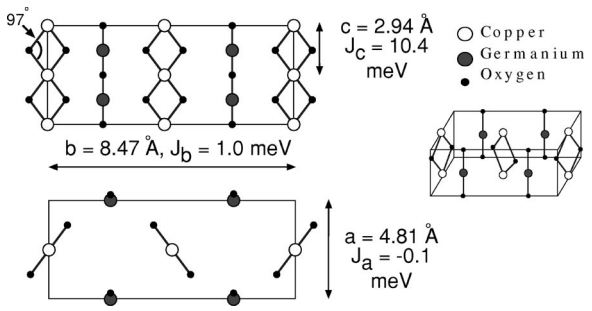

FIG. 1. Structure of $CuGeO_3$.

struct a comprehensive picture of the incommensurate state and the effects of doping on $CuGeO_3$.

II. $CuGeO_3$

$CuGeO_3$ is orthorhombic ($a=4.81$, $b=8.47$, $c=2.94$ Å at room temperature) and consists of CuO_2 chains along the c direction separated by chains of GeO which are displaced along a and b (see Fig. 1). The superexchange between the spin-$\frac{1}{2}$ Cu^{2+} ions through the oxygen bond angle of 97° makes the in-chain coupling antiferromagnetic with $J_c = 10.4$ meV. The couplings along a and b are -0.1 meV and 1.0 meV, respectively.[9] The spin coupling is also very nearly Heisenberg.

$CuGeO_3$ is easily doped with a large range of different ions. Zn^{2+} and Mg^{2+} (both $S=0$) and Ni^{2+} ($S=1$) go in substitutionally for Cu^{2+} and dilute the magnetism of the chains directly. Si^{4+} can be also added in place of Ge^{4+}. The doped Si ions distort the lattice and the configuration of oxygens around the copper sites enough to reverse the coupling from antiferromagnetic to ferromagnetic.[10] This disrupts the antiferromagnetic interaction even more effectively than in-chain dilution, since the Si ions can affect two neighboring oxygen bonds.

No matter which dopant is used, the resulting zero-field phase diagram retains the same overall topology. This zero-field phase diagram has been extensively characterized by several experimental investigations.[11–15] As doping is increased, the spin-Peierls transition temperature decreases. In addition, an antiferromagnetic phase (Néel phase) appears, with a transition temperature which increases with increasing x. At $x \approx 0.023$, which is referred to as the critical concentration, the spin-Peierls state no longer attains long-range order. Heuristically, the dopants remove a spin, making it unavailable for pairing, and thereby inducing an antiphase boundary in the spin-Peierls ordering. If the region between two neighboring impurities contains an odd number of Cu sites, there is also one unpaired spin remaining, which is a mobile soliton. At low enough temperature, these solitons can order with respect to each other; this is the Néel state (see Fig. 2).

While the zero-field phase diagram is essentially the same for all dopants,[16] the uniformity and accuracy of doping that can be achieved varies dramatically among the different dopings. Mg is generally the easiest dopant to use as it substitutes uniformly and very close to the intended concentrations as grown. It was with this in mind that we chose to use

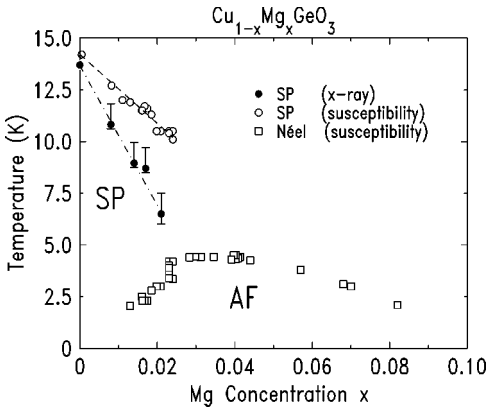

FIG. 2. Zero-field phase diagram of Mg-doped $CuGeO_3$, reprinted from Wang *et al.* (Ref. 12).

Mg-doped samples for our studies of doped $CuGeO_3$ in a magnetic field.

III. EXPERIMENT

We took data on a series of six $Cu_{1-x}Mg_xGeO_3$ crystals: $x=0.0$, 0.004, 0.008, 0.017, 0.021, and 0.023. The crystals were all grown by the floating-zone method at the University of Tokyo, and the level and uniformity of doping were characterized using inductively coupled plasma–atomic emission spectra. All of the samples were found to be uniform to $x \pm 0.001$.

Data were taken at the X20A beamline at Brookhaven National Laboratory's National Synchrotron Light Source. The x-ray beam was vertically focused by a grazing incidence mirror, and an energy of 8 keV was selected by a vertical double-bounce germanium monochromator. After scattering from the sample, the resolution was improved and noise reduced by scattering from a germanium analyzer into the scintillation counterdetector. Counts were normalized using an ion chamber monitor placed after the monochromator.

We used a horizontal scattering geometry to accommodate the 13-T Oxford split-pair superconducting magnet. Scans were taken around the $(H\ K\ L)=(3.5\ 1\ 2.5)$ spin-Peierls reflection to optimize the intensity and minimize the critical field, which is lowest along the b direction. Due to the inability to adjust the out-of-plane angle, the c axis was placed in the scattering plane, and the transverse scans (perpendicular to the chains) shown in this work were taken along the $(3.5\ K\ K)$ direction, which also lays in the scattering plane.

IV. $CuGeO_3$ IN A MAGNETIC FIELD

A mean-field analysis of the spin-Peierls transition[1] gives a linear relation between the zero-temperature spin-Peierls gap and the zero-field transition temperature: $\Delta_0 = 1.765 T_{sp}(0)$. In addition, the mean-field results show a linear relation between the critical field at zero temperature and the zero-field transition temperature $\mu_B H_c = 0.75 k_B T_{sp}(0)$. These results can be refined[1] with the findings of Cross and Fisher[17] giving $\mu_B H_c = 0.69 k_B T_{sp}(0)$ or with results of Nakano and Fukuyama[18] giving $\mu_B H_c$

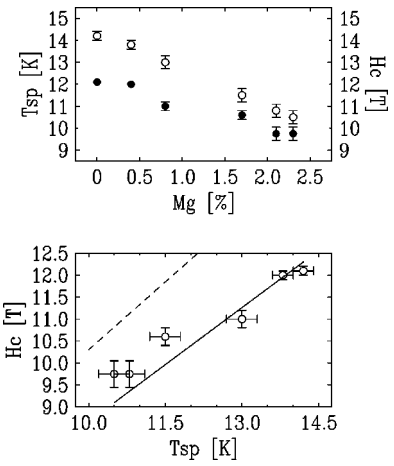

FIG. 3. Top panel shows critical temperatures from susceptibility measurements at $H=1000$ Oe (open circles) and fields corresponding to the onset of x-ray incommensurate peaks at 4 K (filled circles). The bottom panel shows these quantities plotted against each other. The solid line is the best fit to a linear relation with the intercept forced to zero, the dashed line is the prediction of Cross and Fisher (Ref. 19).

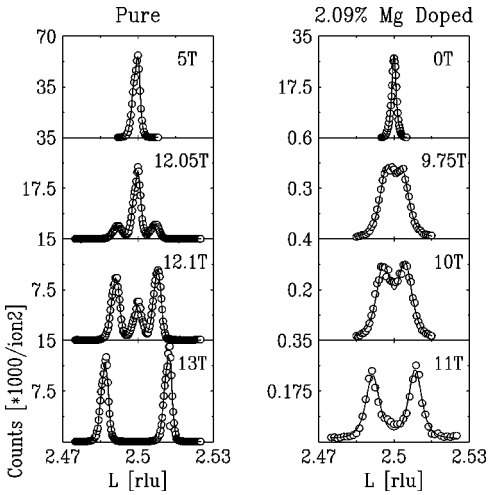

FIG. 4. L scans through the spin-Peierls peak position for various fields crossing the transition at 4 K. The solid lines are the results of fits to a Lorentzian-squared cross-section convolved with the measured instrumental resolution.

$=0.14k_BT_{sp}(0)$. Above the commensurate-incommensurate (C-I) transition, Cross[19] predicted that the peak splitting along the chain direction L should be linearly proportional to the applied field H: $\Delta L=2g\mu_BH/\pi J_cc$.

Figure 3 shows the critical field and zero-field spin-Peierls transition temperatures for our samples. Both the critical temperature and critical field appear to be essentially linear over the range of dopings, and hence linear with respect to each other in agreement with mean-field theory. The best fit to a linear relation between μ_BH_c and k_BT_{sp} gives a proportionality constant of 0.58 ± 0.01. This is intermediate between the values predicted with Cross and Fisher and with Nakano and Fukuyama. The dashed line in the figure shows the prediction for the Cross and Fisher results, while the prediction of Nakano and Fukuyama is off scale.

The transition temperatures shown are from the susceptibility measurements of Fig. 2 and represent the onset temperature for short-range spin-Peierls order at 1000 Oe. The x-ray measurements from the same figure show the onset of long-range order, which has a much stronger dependence on doping than either the short-range order onset or the critical field. It is not possible to find a zero-intercept linear relation between the critical field and the onset of long-range order.

The left-hand side of Fig. 4 shows our scattering results for the (3.5 1 2.5) spin-Peierls peak in pure $CuGeO_3$ as we raise the field across the C-I transition with the temperature fixed at 4 K. Two features are evident here: the system displays coexistence between the dimerized phase and the incommensurate phase over a narrow range of fields, and the incommensurability ΔL onsets at a non-zero value. Both of these observations are clear signals of a first-order transition. We also qualitatively confirm the hysteresis seen in the magnetostriction data for pure samples.[20]

The right-hand side of Fig. 4 shows scans along L through the reciprocal space position (3.5 1 2.5) as the field is raised through the transition for a sample with 2.1% Mg. Since there is never any clear three-peak structure, there is no longer any obvious coexistence of the spin-Peierls phase with the incommensurate phase. Instead, the spin-Peierls peak decreases in amplitude with increasing field and broadens until it splits into two incommensurate peaks. While it is difficult to rule out the existence of a small central peak, and hence the possibility of a coexistence region, certainly the continuous nature of the progression from a single peak to a pair of satellites indicates a transition which is more second order in character.

The widths of the peaks as well as the incommensurability were extracted from fits to a structure factor containing a central commensurate spin-Peierls peak and two incommensurate satellite peaks. For low dopings, coexistence was obvious and three peaks were fit in the transition region. For higher dopings, two peaks were sufficient to obtain good fits, though even at the highest doping, the existence of a small central peak could not be ruled out. For the intermediate doping of 1.71% both two- and three-peak fits were attempted in the transition region, and it was difficult to distinguish which gave the better fit. To avoid ambiguity, we present no data very close to the transition for that sample.

The peaks at higher dopings were not resolution limited, and it was therefore both possible and necessary to choose a specific line shape for fitting the peaks. Previous studies had shown that the peak shape at zero field was consistent with a Lorentzian-squared line shape, reminiscent of the scattering profiles in random-field and spin-glass systems.[12] Our data for fields below the incommensurate transition confirm this. Above the critical field, a Lorentzian-squared line shape convolved with the experimental resolution yields a better fit to the superlattice peaks than a simple Lorentzian convolved with the resolution (Fig. 5). We therefore fit all of our data to a Lorentzian squared convolved with the measured experimental resolution.

Perhaps the best evidence of the change in the nature of the transition can be seen in the incommensurability as a function of field for the various doped samples. Figure 6

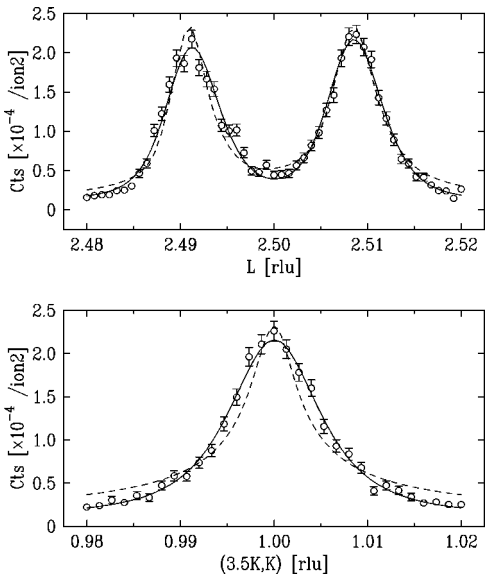

FIG. 5. Results of fits to data for the 2.1% sample at 11 T and 4 K. The solid line is a Lorentzian squared, while the dashed line is a simple Lorentzian.

shows the field dependence of the incommensurability for all the samples we studied. As the doping level rises, increasing the number of soliton pinning sites, the transition moves to lower field. In addition, the transition becomes more gradual, presumably reflecting the crossover to a second-order character of the transition. Of particular interest, we can trace the decrease in the onset incommensurability as the doping increases. In the lower doping samples, the incommensurate peaks first appear at a well-resolved nonzero distance from the spin-Peierls peak, while for the three highest doping samples we cannot distinguish the initial incommensurate peaks from the broadened spin-Peierls peak.

The dashed line in Fig. 6 shows Cross' prediction for the linear dependence of the incommensurability on field. Obviously, the data are not described well by Cross' prediction, though at higher fields, which are inaccessible with our 13-T magnet, the incommensurability could approach this prediction. Buzdin *et al.*,[21] in an effort to improve upon Cross' work, dealt with the transition in the framework of the *XY* model. They arrived at a formula for the incommensurability above a weakly first-order transition:

$$\Delta L = \frac{\pi \Delta_0}{2 v_s \ln(4/\gamma)}, \tag{1}$$

where γ is defined by

$$(H - H_c)/H_c = \gamma^2 \ln(4/\gamma)/2 \tag{2}$$

and $v_s = \pi J_c c/2$.

The solid lines in Fig. 6 represent the results of fits to Buzdin *et al.*'s prediction. For the pure sample, the spin-Peierls gap Δ_0 is taken to be fixed at the value 2.05 meV,[9] and the critical field is fit. The fit is quite good away from the transition, and neutron-scattering results which overlap with our data show agreement with Buzdin *et al.*'s form up to 14.5 T.[22] However, in order to fit our data, the critical field had to be taken at a value of 12.08 T, which is slightly higher than the field at which we see the onset of the incommensurate peaks (12.0 T). It is not surprising that Buzdin *et al.*'s theory should fail very close to the transition, or that our data should also differ from data taken in other experiments very near the transition, since the behavior around the transition field would likely depend on the characteristics of the particular sample in consideration, and on the exact alignment of the magnetic field.

For the doped samples, both the critical field and the spin-Peierls gap were fit. The spin-Peierls gap obtained from the fits decreases rapidly with increased doping, and the quality of the fits, which is good for the lowest doping sample, deteriorates quickly. Since Buzdin's prediction was based on the existence of a (weakly) first-order transition, it is not really surprising that the agreement is poor at the higher dopings, where the transition appears to be continuous. Also, many authors[23,24] have predicted an effective decrease of the spin-Peierls gap with doping, which would agree with the results of these fits. Other indirect evidence of this effect has been seen[25,26] but no direct experimental measurement has confirmed this.

One last note on Fig. 6: we have included in this figure data of Kiryukhin *et al.* for the incommensurability of Ni- and Zn-doped samples taken with the same scattering configuration.[8] As mentioned above, at zero field the effects of doping on the overall topology of the phase diagram do not appear to depend upon the choice of dopant. However, it seems unlikely that, in a field, magnetic and nonmagnetic ions would have the same effect upon the system. The data for the 1.5% Zn sample lie very close to our data for the 1.7% Mg doping, which is reassuring, since both Zn and Mg are nonmagnetic. However, the data for the 2% Ni doping, where Ni^{2+} has spin 1, lie significantly above the 2.1% Mg data. While it is possible that the electron probe microanalysis (EPMA) measured doping for the Ni sample is not a perfectly accurate measure of the actual doping level, it is

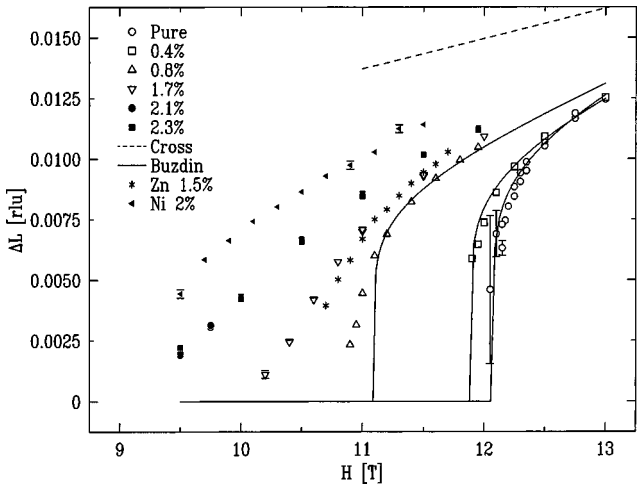

FIG. 6. Incommensurability for all samples at 4 K. The data for the Zn- and Ni-doped samples are from Kiryukhin *et al.* (Ref. 8). Lines are the results of fits to Buzdin *et al.*'s (Ref. 21) Eq. (1) as described in the text.

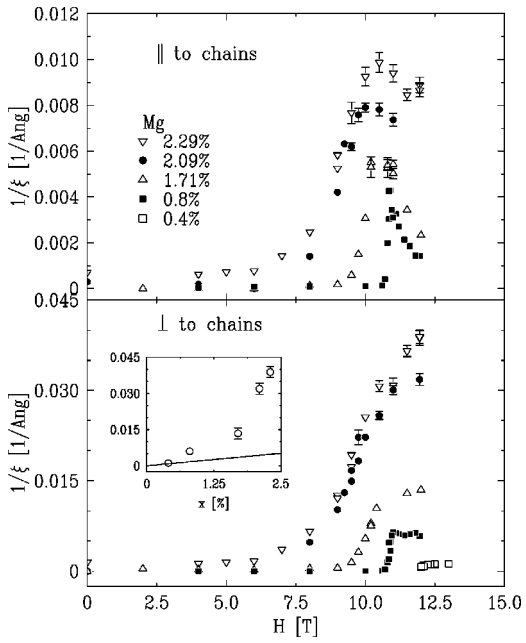

FIG. 7. Transverse and longitudinal widths of the spin-Peierls (below H_c) and incommensurate (above H_c) peaks at 4 K. The inset shows the approximate saturation values for the transverse inverse correlation length. The line is the interdopant spacing.

unlikely that the actual doping would be significantly higher, which would be necessary to reconcile the data for the two different samples. It is possible that the magnetic dopants pin the incommensurate phase more effectively than the nonmagnetic ions, thus stabilizing it at a lower field. However, a more complete study comparing different Cu-site dopants is necessary before definitive conclusions can be drawn.

As mentioned previously, at zero field the spin-Peierls transition temperature decreases with increasing doping until, at a critical concentration of around 2.1%, the spin-Peierls dimerization no longer achieves three-dimensional long-range order. Similarly, we confirm and expand upon the previously reported results[8] showing broadening of the incommensurate peaks at high dopings.

Figure 7 shows the longitudinal (along the chain) and transverse (perpendicular to the chain) widths of the spin-Peierls and incommensurate peaks for the various dopings. There is a large increase in the peak width across the transition, showing that the incommensurate phase is more sensitive to doping than the spin-Peierls phase. Our lowest doping sample already shows broadening in the transverse direction in the incommensurate phase, and the width of the peaks along both directions increases dramatically as the doping increases. For the lowest dopings (not shown on the plot), we were unable to resolve the longitudinal width of the peaks, which implies that the limiting correlation length is longer than 2000 Å.

A naive approach would predict that the correlation length of the incommensurate phase should be of the same length scale, and proportional to, the interdopant spacing.[27] For 0.8% doping, there should be one dopant per 125 lattice spacings along the c direction. The correlation length for the 0.8% sample along the L direction is significantly longer than this. Clearly there is some communication along the chain direction around the dopants due to the structural three-dimensional interactions between the chains. Unfortunately, even at the highest field, the L width in all of the samples was still decreasing with increasing field as we moved farther from the transition, making it impossible to extract a number for the limiting high-field correlation length. This also precludes the determination of the doping dependence of the limiting correlation lengths.

It is interesting to note the different behavior of the correlation length along and transverse to the chains. Both show clear signs of an increasing width below the transition. However, above the transition, the correlation length along the chain begins increasing again, while the correlation length transverse to the chain appears to level off with increasing field. The inset for Fig. 7 shows the values for the transverse inverse correlation length at the highest-field value for each sample. For the lower doping samples, this appears to be the saturation value. In contrast to the longitudinal correlation length, the transverse correlation length appears to be significantly shorter than the interdopant spacing.

V. NÉEL STATE

The character of the Néel ordering in the incommensurate spin-Peierls state is not yet well understood. At low field, the spins associated with the doping-induced solitons order with respect to each other, but to first approximation the solitons do not participate in the spin-Peierls ordering so long as the structure remains commensurate. At high field, however, the doping-induced solitons may be involved in the ordering of the incommensurate phase, contributing to the decrease in critical field which is seen with increasing doping.

Since the Néel state involves no additional structural distortion, we could not probe the peak corresponding to the ordering directly with structural x-ray scattering. However, as temperature is lowered, the width of the spin-Peierls and satellite peaks begins to increase, corresponding to a decrease in the correlation length ξ. Previous results[13,15] at zero field show that this is an indication of the onset of Néel ordering. Hereafter, we define T_N as the temperature below which the correlation length is suppressed. Since we were able to take data down to 1.6 K, we could see this effect in all of the doped samples except for the 0.4%. The most complete data were taken on the 2.1% sample.

As a case study, we wished to make a complete characterization of the Néel state for a single doping sample. We chose to do this for the 2.1% sample, since this sample (which has a concentration very close to the critical concentration at zero field) had the highest Néel transition while still maintaining a resolution-limited peak at zero field, hence allowing us to make an accurate determination of the resolution function.

For a series of fields from zero up to 13 T, we took scans though the (3.5 1 2.5) position (and satellite positions). The sample was zero-field cooled, the field was raised to the appropriate value, and data were taken upon raising the temperature from base temperature (1.6 K) to the paramagnetic transition. After each cooling we generally waited between

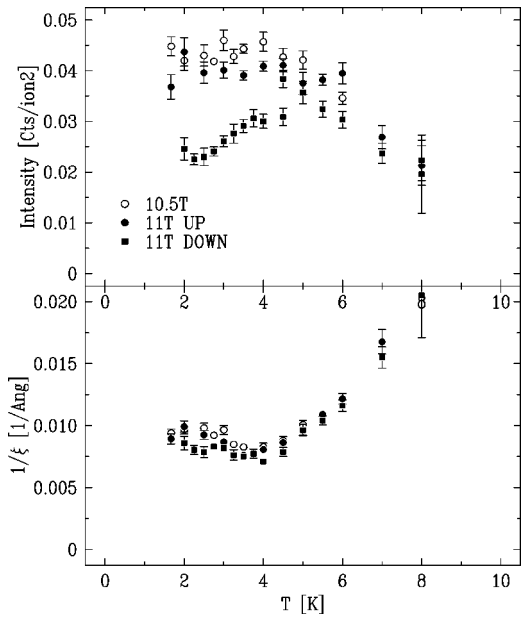

FIG. 8. Integrated intensities and inverse correlation lengths along the chain direction for zero-field cooling and increasing temperature at various fields above the critical field for the 2.1% sample.

15 and 30 min to stabilize the low-temperature phase before taking data, as per the findings of Wang *et al.* that the time scale of metastability for the low-temperature phase was of approximately this order of magnitude.[12] We should note that, due to the time necessary to raise the field, the wait before collecting data was longer for higher-field data than for lower field. This time was on the order of 10–20 min for the lower fields, and ranged up to an hour or more for the highest fields.

Above the critical field (Fig. 8) the behavior of the incommensurate peaks at the Néel transition is nearly identical to that seen in the spin-Peierls peak at lower field. However, it does seem that the onset temperature of the Néel ordering moves higher, probably because of the presence of additional solitons. Figure 8 also shows the hysteresis of the Néel transition upon cooling back through the transition. This behavior is very similar to that seen in zero field by other experimenters.[12] The integrated peak intensity is very nearly constant upon heating, though scans taking upon cooling show a decrease in peak intensity (also seen in previous zero-field studies).

In addition to the temperature-dependent data shown above, we took three field scans at 2, 3, and 4 K (i.e., below, at, and above the Néel transition). These scans showed essentially the same behavior. Figure 9 shows the complete phase diagram for the 2.1% sample which was deduced from these measurements. The dashed line indicates the approximate location of the incommensurate phase boundary. There is no clear transition from the incommensurate phase to the high-temperature uniform phase. Rather, with increasing temperature at fixed field, we observe a slow increase of the width of the peaks together with a decrease of both the intensity and the incommensurability.

Due in large part to the effects of metastability, and the inability to observe the Néel state directly, it is difficult to draw any unambiguous conclusions. However, very generally we can say that the subtle increase in the Néel temperature above the transition field indicates that the incommensurate state is more unstable to the formation of uniform Néel ordering than is the dimerized spin-Peierls state. However, the nearly flat integrated intensity upon zero-field cooling indicates that the strength of the local structural ordering in both the dimerized state and the incommensurate state is essentially unaffected by the Néel ordering. Rather the structural state merely breaks up into smaller domains.

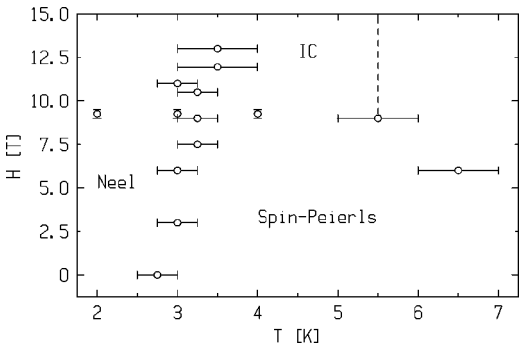

FIG. 9. Experimentally determined phase diagram for the 2.1% Mg-doped sample. The dashed line indicates the approximate location of the high-temperature limit for the incommensurate phase.

VI. THIRD HARMONICS

The naive picture of the incommensurate state as a lattice of discrete flipped spins is more complicated in reality. Both the magnetic and structural ''solitons'' are actually accompanied by a much longer-range distortion of the surrounding order. Many calculations have been performed concerning the shape of the solitons in the incommensurate phase. In particular, quantitative predictions for the soliton width exist for pure $CuGeO_3$.[1] The soliton width is a parameter which describes the extent of the soliton, and, when compared with the periodicity of the superlattice, this quantity can give some idea of whether the modulation of the lattice is discrete or sinusoidal. The soliton width can be extracted from a measurement of the intensity of the third harmonic peaks of the incommensurate state. The higher-order Fourier components are sensitive to the shape of the modulation, being minimum for a pure sine wave, and maximum for a square-wave distortion. Kiryukhin *et al.*[8] measured the third harmonic intensity for pure $CuGeO_3$ and arrived at a value for Γ of $13.6c$. The calculated value, using a field-theory description of the nearest-neighbor Heisenberg model, is $\Gamma/c = v_s/\Delta_{sp} = 8.0$,[18] which is significantly smaller than the value deduced from the x-ray measurements, and therefore indicates a much less sinusoidal soliton shape.

We attempted to measure the third harmonic scattering in our doped samples. In all of the samples but the lowest doping (0.4%) and pure samples, the third harmonic intensity was too weak to measure (less than 1/1000 of the incommensurate peak). We performed thorough measurements of the pure and 0.4% samples, with some unexpected results.

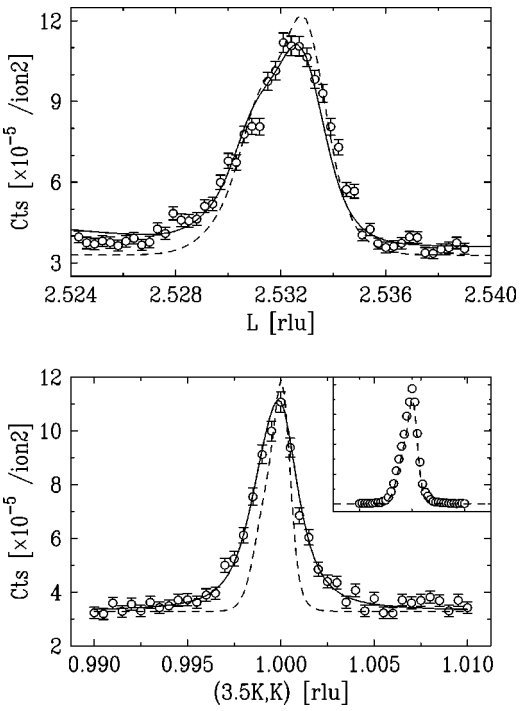

FIG. 10. Scans through the third harmonic peak for $H=12.5$ T, $T=4$ K. The solid lines are the results of fits used to extract the soliton width. The dashed lines show resolution-limited fits (the asymmetry in the L scan is from mosaicity). The inset in the bottom panel shows the resolution-limited transverse scan ($0.995<K<1.005$) through the first harmonic.

Figure 10 shows the third harmonic scans in pure $CuGeO_3$ at 4 K and 12.5 T. The third harmonic is well defined and resolution limited along the chain direction, as one would expect. However, as shown in the lower panel of the figure, the transverse ($3.5\ K$, K) scan through the third harmonic is broadened, though the first harmonic peak is resolution limited in this direction (see inset) as well as in the longitudinal direction. This broadening was not observed in previous x-ray scattering studies, mostly due to a much lower signal, which limited the amount of data that could be taken on the third harmonics.

It is not unusual that the first and third harmonic orderings should have different characteristic length scales. Studies of smectic liquid crystals[28] show a similar broadening of the higher harmonic scattering with respect to the first harmonic. Subsequent theoretical calculations[29,30] were able to account for the observed correlation length ratio for that system. This theory is not easily adaptable to our system. Nevertheless, on a quite general basis it is evident that the observation of a nonzero width in the third harmonic peak requires a nonzero width of the first harmonic. We can therefore conclude that the incommensurate phase in nominally ''pure'' $CuGeO_3$, though of a correlation length long enough to appear resolution limited (greater than 2000 Å), is in fact not long-range ordered transverse to the chain direction.

The most likely explanation for this is that there exists in any real sample some quantity of impurities and imperfections. The ''pure'' sample must in fact be considered to be a very low doping sample. This is consistent with the fact that

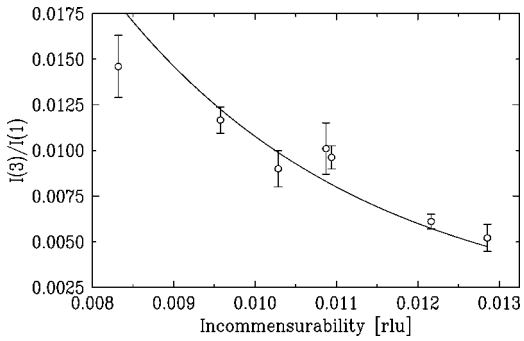

FIG. 11. Ratio of the integrated intensities of the first and third harmonics of the incommensurate ordering in pure $CuGeO_3$ at 4 K. The solid line is the result of a fit to a constant soliton width from Eq. (4).

T_{SP} at zero field varies among nominally stoichiometric $CuGeO_3$ samples. Our measurements therefore indicate that in the direction perpendicular to the chains, the incommensurate phase in $CuGeO_3$ is critical, in the sense that any amount of disorder will disrupt the long-range order.

The broadening of the third harmonic in the transverse direction has the additional effect of increasing the integrated intensity from that found if the transverse scan is assumed to be resolution limited, as it was in Kiryukhin *et al.*'s work.[8] We therefore took a series of measurements of I_3/I_1 as a function of field and compared it to the relation between Γ and the incommensurability:

$$\pi/\Delta L = 2kK(k)\Gamma, \tag{3}$$

$$I_3/I_1 = \left(\frac{Y}{Y^2+Y+1}\right)^2, \tag{4}$$

$$Y = \exp[-\pi K(\sqrt{1-k^2})/K(k)], \tag{5}$$

where K is the complete elliptic integral of the first kind and k is a parameter between 0 and 1 which describes the soliton shape. This form assumes a shape to the soliton which is described by[18]

$$u(l) = \epsilon(-1)^l \mathrm{sn}(lc/\Gamma k, k) \tag{6}$$

at lattice site l, where $\mathrm{sn}(x,k)$ is a Jacobi elliptic function. The parameter k was found from the ratio of the intensities, and Γ was then found from k and the incommensurability. Assuming Γ constant with field we arrived at a best-fit value of $11.2\pm0.3c$ (see Fig. 11). This is smaller than the value found by Kiryukhin *et al.* due to the increase in third harmonic intensity from the broadening. However, our value is still larger than the value of $8c$ predicted by theory.

Other determinations of Γ have been made with neutron scattering which gives a minimum value of $9.15\pm0.14c$,[22] and NMR, which gives values between 6 and $10c$.[31] It must be noted that the x-ray measurements see the structural soliton width, while this neutron-scattering measurement was of the magnetic soliton width. These quantities are not necessarily identical,[32] and in fact are predicted to occur in the ratio: $\Gamma_d/\Gamma_m = 1.24$. The corresponding structural soliton

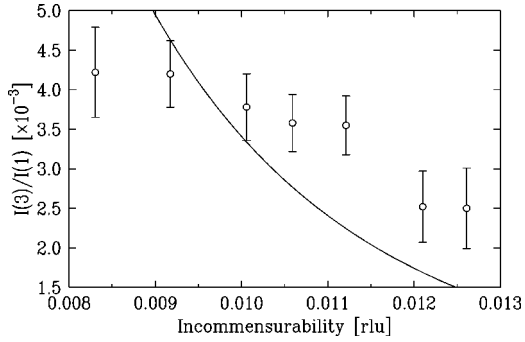

FIG. 12. Ratio of the integrated intensities of the first and third harmonics of the incommensurate ordering in 0.4% Mg-doped $CuGeO_3$ at 4 K. The solid line is the result of a fit to a constant soliton width from Eq. (4).

width from the minimum neutron scattering measurement would then be $11.35c$, which is very close to the value of 11.2 derived from our measurements.

The soliton width has also been predicted by numerical density-matrix renormalization-group calculation to change close to the transition,[32] and this has been measured in the same neutron-scattering experiment mentioned above. The neutron investigators observed a quick drop of Γ from $11.5c$ near H_c to a minimum of $9.15c$ occurring at around 13 T. We do not see clear evidence of such an evolution, and, though the point nearest to the transition appears to have a larger Γ (around $12.1c$) than the rest of the data, this value is significantly smaller than 1.24 times the neutron-scattering value closest to the transition, despite our point being 0.2-T closer to H_c.

Our measurements on the 0.4% sample showed a similar broadening of the third harmonic with respect to the first harmonic in the transverse direction (the longitudinal direction was again resolution limited). In this case, however, the first harmonic was also not resolution limited, allowing us to measure $\xi_3/\xi_1 = 8.4 \pm 1.95$ at $T = 4$ K and $H = 13$ T. Assuming that this quantity is not field or temperature dependent, we used this number with our longitudinal scans to again plot I_3/I_1 versus field. The value for Γ which we extracted is $15.7 \pm 0.3c$. However, as one can see in Fig. 12, for this doping the fit to a constant Γ is very poor. The trend seems to be for increasing Γ as H gets closer to H_c, which is in qualitative agreement with the field dependence seen in the neutron-scattering studies of the pure material.

One thing which is definitely clear from our measurements is that the soliton width in the 0.4% doped sample is significantly larger than that in the pure sample. Some of this may be attributed to a contribution from the static Debye-Waller factor. Following data from a computer modeling of strong impurity pinning,[8] we would expect that 0.4% impurities would result in a suppression of $I(3)/I(1)$ by a factor of about 0.8. If we correct for this, we arrive at a value of $\Gamma = 14.5 \pm 0.4c$, which is still greater than that of the pure sample. It appears, therefore, that another effect of the impurities is to smooth out the displacements that result from the soliton lattice making it more sinusoidal. 0.4% is a very small doping level, so this effect happens very quickly, which then makes it clear why we were unable to observe the higher harmonic peaks in any of the higher doping samples.

VII. DISCUSSION

One interpretation of the universality of doping effects on the zero-field $CuGeO_3$ phase diagram is based on the assumption that all of the dopants generate effective ''random fields'' for the various sites in the chains. In fact, the original theoretical discussion of random fields by Imry, Ma, and Aharony[33,34] specifically mentions doped systems with a structurally distortive transition as an example of an experimentally realizable random-field system. The random distribution of impurities surrounding a given lattice site creates a site-specific strain field. An alternative approach involves a structural spin-glass model arising from competing short and long-range interactions. The experimental ramifications of such a model are closely similar to those of the random-field model.

As was the case for the zero-field experiments, our data for the incommensurate state shows evidence of random-field effects. The first indication of this was in the Lorentzian-squared line shape for the incommensurate peaks, indicating exponentially decaying correlations, as had been observed previously in the doped spin-Peierls phase[12] as well as in the earlier studies of the incommensurate phase.[8]

Early in the theoretical discussion of the random-field model, a heuristic analysis appeared in the literature predicting that temperature-driven first-order phase transitions should become second order under the influence of random fields.[35] While the exact argument in that paper is not directly relevant to a field-driven transition, it was based on very general principles. Specifically, the discussion was focused on the distribution of critical temperatures caused by the statistical variation of impurities in a given sample volume and the resulting interfacial energy from having some of the sample in the new phase while neighboring sections are not. These general concepts should also be applicable to a field-driven transition, and hence the end result should be the same. However, due to the lack of a specific theoretical analysis for field-driven transitions in random-field systems, there remain some unanswered questions for our system. The first is whether there should be a nonzero doping above which the transition becomes second order, or if an infinitesimal doping will cause the change in the nature of the transition. Equivalently, it is not known whether or not there is a tricritical point at some nonzero doping. In addition, it is unknown whether the first-order transition will be destroyed for all dimensions, or if there is a critical dimension. Analysis of multicritical systems with bond randomness[36] (as opposed to random fields) have shown that for $d > 2$ there is a threshold doping for destruction of the first-order transition, while for $d \leqslant 2$ infinitesimal randomness is sufficient. Since we see definitive coexistence for $CuGeO_3$ up to 0.8%, this system seems to have a threshold doping for the conversion of the phase boundary to second order. This argues for a tricritical point model for the phase diagram.

Another characteristic effect of random fields is the destruction of true long-range order for arbitrarily small doping

in continuous order-parameter systems for $d \leqslant 4$ and for Ising systems with $d \leqslant 2$. As was mentioned above, we see critical destruction of long-range order in the three-dimensionally ordered incommensurate phase. This is consistent with the fact that the incommensurate phase has XY symmetry, and is in contrast with the three-dimensionally ordered Ising spin-Peierls phase which has a critical concentration of 2.3%.

VIII. CONCLUSIONS

Our study of the incommensurate phase in doped $CuGeO_3$ has yielded some interesting results. The doped incommensurate phase displays many of the classic traits of a random field, continuous order-parameter system. We observe Lorentzian-squared line shapes, destruction of long-range order with infinitesimal doping, and the conversion of a first-order transition to a second-order transition.

We have also performed a more accurate determination of the structural soliton width in pure $CuGeO_3$, as well as making the first x-ray measurement of the soliton width in a doped sample. Both samples show a difference between the correlation length of the first and third harmonic scatterings, similar to what is seen in smectic liquid crystals. Doping quickly reduces the third harmonic scattering, indicating a drastic effect on the shape of the lattice modulation.

ACKNOWLEDGMENTS

This work was supported by the NSF under Grant Nos. DMR0071256 and DMR-0093143 and by the MRSEC Program of the National Science Foundation under Grant No. DMR98-08941. The work at Brookhaven National Laboratory was carried out under Contract No. DE-AC02-98CH10886, Division of Materials Science, U. S. Department of Energy. Research at the University of Toronto is part of the Canadian Institute for Advanced Research and is supported by the Natural Science and Engineering Research Council of Canada. Research at the University of Tokyo was partially supported by a Grant-in-Aid for COE Research, the ''SCP Project,'' from the Ministry of Education, Sports, Science and Technology, Japan.

[1] J. W. Bray, in *Extended Linear Chain Compounds*, of The Spin-Peierls Transition, edited by J. S. Miller (Plenum, New York, 1983), Vol. 3, Chap. 7, p. 353.
[2] M. Hase, I. Terasaki, Y. Sasago, K. Uchinokura, and H. Obara, Phys. Rev. Lett. **71**, 4059 (1993).
[3] M. Hase, I. Terasaki, K. Uchinokura, M. Tokunaga, N. Miura, and H. Obara, Phys. Rev. B **48**, 9616 (1993).
[4] Q. Harris, Q. Feng, R. Birgeneau, K. Hirota, K. Kakurai, J. Lorenzo, G. Shirane, H. Kojima, I. Tanaka, and Y. Shibuya, Phys. Rev. B **50**, 12 606 (1994).
[5] Q. Harris, Q. Feng, R. Birgeneau, K. Hirota, G. Shirane, M. Hase, and K. Uchinokura, Phys. Rev. B **52**, 15 420 (1995).
[6] M. Hase, I. Terasaki, and K. Uchinokura, Phys. Rev. Lett. **70**, 3651 (1993).
[7] V. Kiryukhin and B. Keimer, Phys. Rev. B **52**, R704 (1995).
[8] V. Kiryukhin, B. Keimer, J. Hill, S. Coad, and D. Paul, Phys. Rev. B **54**, 7269 (1996).
[9] M. Nishi, O. Fujita, and J. Akimitsu, Phys. Rev. B **50**, 6508 (1994).
[10] W. Geertsma and D. Khomskii, Phys. Rev. B **54**, 3011 (1996).
[11] T. Masuda, A. Fujioka, Y. Uchiyama, I. Tsukada, and K. Uchinokura, Phys. Rev. Lett. **80**, 4566 (1998).
[12] Y. Wang, V. Kiryukhin, R. Birgeneau, T. Masuda, I. Tsukada, and K. Uchinokura, Phys. Rev. Lett. **83**, 1676 (1999).
[13] V. Kiryukhin, Y. Wang, S. LaMarra, R. Birgeneau, T. Masuda, I. Tsukada, and K. Uchinokura, Phys. Rev. B **61**, 9527 (2000).
[14] T. Masuda, K. Ina, K. Hadama, I. Tsukada, K. Uchinokura, H. Nakao, M. Nishi, Y. Fujii, K. Hirota, G. Shirane, Y. Wang, V. Kiryukhin, and R. Birgeneau, Physica B **284**, 1637 (2000).
[15] H. Nakao, M. Nishi, Y. Fujii, T. Masuda, I. Tsukada, K. Uchinokura, K. Hirota, and G. Shirane, J. Phys. Soc. Jpn. **68**, 3662 (1999).
[16] T. Masuda, I. Tsukada, K. Uchinokura, Y. Wang, V. Kiryukhin, and R. Birgeneau, Phys. Rev. B **61**, 4103 (2000).
[17] M. Cross and D. Fisher, Phys. Rev. B **19**, 402 (1979).
[18] T. Nakano and H. Fukuyama, J. Phys. Soc. Jpn. **49**, 1679 (1980).
[19] M. Cross, Phys. Rev. B **20**, 4606 (1979).
[20] B. Buchner, T. Lorenz, R. Walter, H. Kierspel, A. Revcolevschi, and G. Dhalenne, Phys. Rev. B **59**, 6886 (1999).
[21] A. Buzdin, M. Kulic, and V. Tugushev, Solid State Commun. **48**, 483 (1983).
[22] H. Ronnow, M. Enderle, D. McMorrow, L. Regnault, G. Dhalenne, A. Revcolevschi, A. Hoser, P. Vorderwisch, and H. Schneider, Physica B **276**, 678 (2000).
[23] M. Saito and H. Fukuyama, Physica B **284**, 1565 (2000), and references therein.
[24] G. Martins, E. Dagotto, and J. Riera, Phys. Rev. B **54**, 16032 (1996).
[25] J. Takeya, I. Tsukada, Y. Ando, T. Masuda, K. Uchinokura, I. Tanaka, R. Feigelson, and A. Kapitulnik, Phys. Rev. B **63**, 214407 (2001).
[26] J. Lussier, S. Coad, D. McMorrow, and D. Paul, J. Phys.: Condens. Matter **7**, L325 (1995).
[27] S. Bhattacharjee, T. Nattermann, and C. Ronnewinkel, Phys. Rev. B **58**, 2658 (1998).
[28] L. Wu, M. Young, Y. Shao, C. Garland, R. Birgeneau, and G. Heppke, Phys. Rev. Lett. **72**, 376 (1994).
[29] A. Aharony, R. Birgeneau, C. Garland, Y.-J. Kim, V. Lebedev, R. Netz, and M. Young, Phys. Rev. Lett. **74**, 5064 (1995).
[30] R. Netz and A. Aharony, Phys. Rev. E **55**, 2267 (1997).
[31] M. Hortavic, Y. Fagot-Revura, C. Berthier, K. Hirota, P. Segransan, G. Dhalenne, and A. Revcolevschi, Phys. Rev. Lett. **83**, 420 (1999).
[32] G. Uhrig, Physica B **280**, 308 (2000).
[33] Y. Imry and S. Ma, Phys. Rev. Lett. **35**, 1399 (1975).
[34] A. Aharony, Y. Imry, and S. Ma, Phys. Rev. Lett. **37**, 1364 (1976).
[35] Y. Imry and M. Wortis, Phys. Rev. B **19**, 3580 (1979).
[36] A.N. Berker, J. Appl. Phys. **70**, 5941 (1991).